

SANDIA REPORT

SAND2008-3737

Unlimited Release

Printed June 2008

In-situ Time-of-Flight Neutron Diffraction of ErD_2 (β phase) Formation during D_2 Loading

Mark A. Rodriguez, Clark S. Snow, Ryan R. Wixom,
James F. Browning and Anna Lobet

Prepared by
Sandia National Laboratories
Albuquerque, New Mexico 87185 and Livermore, California 94550

Sandia is a multiprogram laboratory operated by Sandia Corporation,
a Lockheed Martin Company, for the United States Department of Energy's
National Nuclear Security Administration under Contract DE-AC04-94AL85000.



Sandia National Laboratories

Issued by Sandia National Laboratories, operated for the United States Department of Energy by Sandia Corporation.

NOTICE: This report was prepared as an account of work sponsored by an agency of the United States Government. Neither the United States Government, nor any agency thereof, nor any of their employees, nor any of their contractors, subcontractors, or their employees, make any warranty, express or implied, or assume any legal liability or responsibility for the accuracy, completeness, or usefulness of any information, apparatus, product, or process disclosed, or represent that its use would not infringe privately owned rights. Reference herein to any specific commercial product, process, or service by trade name, trademark, manufacturer, or otherwise, does not necessarily constitute or imply its endorsement, recommendation, or favoring by the United States Government, any agency thereof, or any of their contractors or subcontractors. The views and opinions expressed herein do not necessarily state or reflect those of the United States Government, any agency thereof, or any of their contractors.

Printed in the United States of America. This report has been reproduced directly from the best available copy.

Available to DOE and DOE contractors from
U.S. Department of Energy
Office of Scientific and Technical Information
P.O. Box 62
Oak Ridge, TN 37831

Telephone: (865) 576-8401
Facsimile: (865) 576-5728
E-Mail: reports@adonis.osti.gov
Online ordering: <http://www.osti.gov/bridge>

Available to the public from
U.S. Department of Commerce
National Technical Information Service
5285 Port Royal Rd.
Springfield, VA 22161

Telephone: (800) 553-6847
Facsimile: (703) 605-6900
E-Mail: orders@ntis.fedworld.gov
Online order: <http://www.ntis.gov/help/ordermethods.asp?loc=7-4-0#online>



SAND2008-3737
Unlimited Release
Printed June 2008

In-situ Time-of-Flight Neutron Diffraction of ErD_2 (β phase) Formation during D_2 Loading

Mark A. Rodriguez (01822), Clark S. Snow (02735), Ryan R. Wixom (02555)
Sandia National Laboratories
P.O. Box 5800
Albuquerque, New Mexico 87185-MS1411

Anna Llobet
Lujan Neutron Scattering Center
Los Alamos National Laboratory
Los Alamos, NM 87545-H805

James F. Browning
Spallation Neutron Source
Oak Ridge National Laboratory
Oak Ridge, TN 77831-6475

Abstract

In an effort to better understand the structural changes occurring during hydrogen loading of erbium target materials, we have performed D_2 loading of erbium metal (powder) with simultaneous neutron diffraction analysis. This experiment tracked the conversion of Er metal to the α erbium deuteride (solid-solution) phase and then on to the β (fluorite) phase. Complete conversion to $\text{ErD}_{2.0}$ was accomplished at 10 Torr D_2 pressure with deuterium fully occupying the tetrahedral sites in the fluorite lattice. Increased D_2 pressure (up to 500 Torr at 450°C) revealed $\sim 10\%$ deuterium occupation of the octahedral sites. Subsequent vacuum pumping of the sample at 450°C removed octahedral site occupancy while maintaining tetrahedral deuterium occupancy, thereby yielding stoichiometric $\text{ErD}_{2.0}$ β phase.

Acknowledgements

The authors would like to acknowledge Jim Browning, formerly of the Applied Science and Technology Maturation (02735) department, for his outstanding help in planning and designing the in-situ reaction chamber used in this study. We would also like to acknowledge the hard work of David Hawn (02735) during the integration phase of the reactor and vanadium heater assembly. His contributions greatly simplified the measurement process. The authors also thank Dan Kammler for his preparation of the Er powder via cryo-milling.

Contents

Introduction	7
Experimental Procedure	10
Results and Discussion.....	13
Conclusions.....	19
References	20

Introduction

The ground-breaking work on the Erbium-Hydrogen system by Lundin documents three possible phases (α , β , γ) for this metal hydride.[1] The α phase can be understood as having the same hexagonal symmetry as that of Er metal, but with the addition of hydrogen into the host Er lattice as a solid-solution. The β phase has a fluorite-type structure and usually occurs near the formula ErH_2 , hence it is also referred to as the dihydride phase. Lundin also documents a tri-hydride phase (γ) which has also been recently explored by Tewell and King.[2] As our interest in this study was monitoring of the formation of ErD_2 from Er metal, we shall limit discussion in this report to the α and β phases.

Synthesis of the β phase via systems such as a PCT Apparatus[3] result in powders and films that traverse the phase diagram for the erbium-hydride system. However, many of the synthesis protocols are based on empirical observations of the final synthesized compounds and little is understood regarding the crystallographic behavior of the α and β phase during hydrogen (i.e. protium, deuterium, and/or tritium) loading. As a means to probe the α and β phase while they are forming, we have undertaken in-situ deuterium loading with simultaneous neutron scattering. We employed D_2 in our analysis as deuterium is scattered well by neutrons and enables our measurements to have sensitivity to deuterium site occupancies in the β phase during the loading process.

Of particular interest in the loading process was the determination of the tetrahedral (D_{tet}) and octahedral (D_{oct}) site occupancies for the β phase. For reference, the ErD_2 structure is shown below in three models (see Figure 1). Model 1, which only contains the Er atoms, shows the face-centered cubic (FCC) framework of the fluorite-type lattice (space group $Fm-3m$) where the Er locates on the (0,0,0) corner site. The FCC symmetry of the fluorite demands additional Er occupation in the faces, that is the $(\frac{1}{2}, \frac{1}{2}, 0)$ site and its equivalent positions. This results in a total of 4 Er atoms within the fluorite unit cell. Model 2 shows the typical location of deuterium atoms relative to the Er positions. The deuterium atoms shown in Model 2 are designated as D_{tet} because they locate on the $(\frac{1}{4}, \frac{1}{4}, \frac{1}{4})$ site and therefore take up a tetrahedral coordination to the neighboring Er atoms. The ratio of site multiplicity is 1:2 for Er: D_{tet} so complete filling of the D_{tet} sites yields the stoichiometry of $\text{ErD}_{2.0}$ or the dihydride phase and the number of formula units per cell (i.e. Z) = 4. There is an additional site location for deuterium which is shown in Model 3. This site, referred to as D_{oct} , is located at the center of the cell $(\frac{1}{2}, \frac{1}{2}, \frac{1}{2})$ and likewise at the equivalent edge site $(0, \frac{1}{2}, 0)$. Note that the D_{oct} site has octahedral coordination when referenced to the nearest 6 Er atoms surrounding this site location, these being the Er atoms in the faces of the cell. But in fact, the nearest neighbor site to the D_{oct} core in the middle of the fluorite structure is the D_{tet} site. The D_{oct} site takes up an 8-fold coordination to the D_{tet} atoms. This information is important in later discussions. Udovic, *et al.* has documented that under certain conditions the D_{oct} site may contain a small fraction of site occupancy.[4]

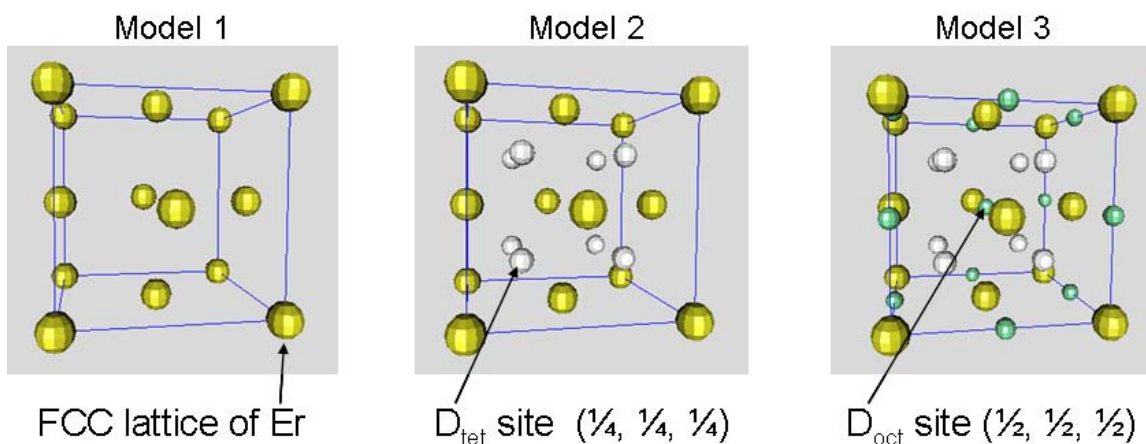


Figure 1. Fluorite (β phase) lattice illustrating the D_{tet} and D_{oct} sites. See text for details.

It is of some benefit to document the reasons for employing neutron diffraction in our analysis. Neutron scattering requires access to large-scale facilities employing either a nuclear reactor, or in the case of neutron spallation sources, a linear particle accelerator and spallation target housing. Access to beam-time at such facilities is very limited and is therefore not considered routine experimentation. In our case we utilized the spallation source at the Lujan Center located at the Los Alamos Neutron Science Center (LANSCE) at Los Alamos National Laboratory. There are two main reasons for employing neutron scattering. These are: 1) penetration depth and 2) deuterium sensitivity. First, with respect to penetration depth, we desired to analyze the loading of D_2 within bulk Er powder. Our specimens were large (several grams) and required a beam that would penetrate through this large sample volume as we desired to know the bulk behavior of D_2 loading and not limit our analysis to surface phenomena. The highly penetrating nature of the time-of-flight (TOF) neutron beam easily addresses this requirement.

The second reason for neutron scattering is the need for sensitivity to deuterium. Crystallographic studies performed in laboratory settings usually employ sealed tube X-ray sources. X-rays scatter well from heavy atoms such as Er because the scattering behavior of an atomic species is proportional to the number of electrons present on the atom. Hydrogen isotopes, with their lone electron are notorious for evading detection using standard X-ray analysis techniques. However, neutron scattering lengths are dictated by their interaction with the nucleus of the scattering atom. As it turns out, the scattering length for deuterium (6.671 fm) is of the same order as that of the Er species (7.79 fm) which means that a neutron scattering measurement will give nearly equal sensitivity to the two atomic species, opening up opportunities to monitor structural parameters such as site occupancy of the deuterium atoms within the α and β phases.

As a means of illustrating deuterium sensitivity, simulated relative peak intensities for various hkl values were generated for the case of neutron diffraction patterns. These peak intensities were based on the three models shown in Figure 1. The results are tabulated in Table 1. From this table we can see that the neutron diffraction pattern changes

dramatically with the addition of D into the D_{tet} sites. Further addition of D to the D_{oct} sites at a 10% site-occupancy shows changes large enough to give confidence regarding experimental sensitivity to the presence of both D_{tet} and D_{oct} in the β phase fluorite structure. Note the sensitivity of the (111) and (311) peaks to the octahedral site occupancy. For comparison purposes we include the calculated intensities expected from analysis using X-ray Diffraction (XRD) in Table 2. Note that the peak intensities in Table 2 are nearly completely dependent on the Er scattering; addition of deuterium makes little or no different in the relative intensities of the reported hkl values.

Table 1. Calculated relative peak intensities for various hkl values based on neutron scattering from models shown in Figure 1.

hkl	d (Å)	I_{rel} (%) Model 1	I_{rel} (%) Model 2	I_{rel} (%) Model 3	Diff. % 3-1
111	2.954	100	26	21	-79
200	2.558	56	6	5	-51
220	1.808	55	100	100	+45
311	1.543	78	20	16	-62
222	1.477	24	3	2	-22
400	1.279	13	24	24	+11
331	1.174	45	12	9	-36
420	1.144	43	5	4	-39
422	1.044	36	67	67	+31

Table 2. Calculated relative peak intensities for various hkl values based on X-ray scattering from models shown in Figure 1.

hkl	d (Å)	I_{rel} (%) Model 1	I_{rel} (%) Model 2	I_{rel} (%) Model 3	Diff. % 3-1
111	2.954	100	100	100	
200	2.558	51	49	49	-2
220	1.808	35	36	36	+1
311	1.543	40	40	40	
222	1.477	11	11	11	
400	1.279	5	5	5	
331	1.174	15	15	15	
420	1.144	13	13	13	
422	1.044	10	10	10	

Experimental Procedure

High purity (99.99%) Er chunks in the size range of 100 μm to 2 mm were used as loose powder so as to obtain a random scattering from the Er and hydrided phases. The random neutron scattering of a loose powder provides a more straightforward analysis of the neutron diffraction datasets. No attempt was made to isolate the Er powder from the air atmosphere prior to loading it into the reaction vessel. Therefore, the Er undoubtedly contained the typical oxide passivation layer on the surface of the individual chunks of the powder sample. Because of the large grain size of the powder specimen, the surface-to-volume ratio is dominated by the Er metal bulk interior of the grains and very little oxygen presence is contributed by the thin (~ 60 Å) passivation layer.

The schematic of the experimental setup is shown in Figure 2. Vanadium is effectively transparent to neutrons; this metal was the logical choice for the heating element. Additionally, the heat shields for the heating element were fabricated from thin vanadium foil. A thermocouple (type K) was placed down into the reaction vessel to measure the temperature of the sample during heating. The thermocouple was placed about 1 mm above the powder Er sample. The gas system employed a roughing pump/turbo pump system that could obtain vacuum conditions of $< 10^{-7}$ Torr throughout the entire gas system. The gas system also employed an isolation valve between the in-situ reactor chamber and the vacuum. This allowed isolation of the system so that various D_2 gas pressures could be applied to the sample in the reactor chamber. Addition of D_2 gas into the reactor was controlled by a small needle valve plumbed in-line between the D_2 cylinder and the in-situ reactor. MKS Baratron pressure gauges were employed to monitor the D_2 pressures applied to the in-situ reactor.

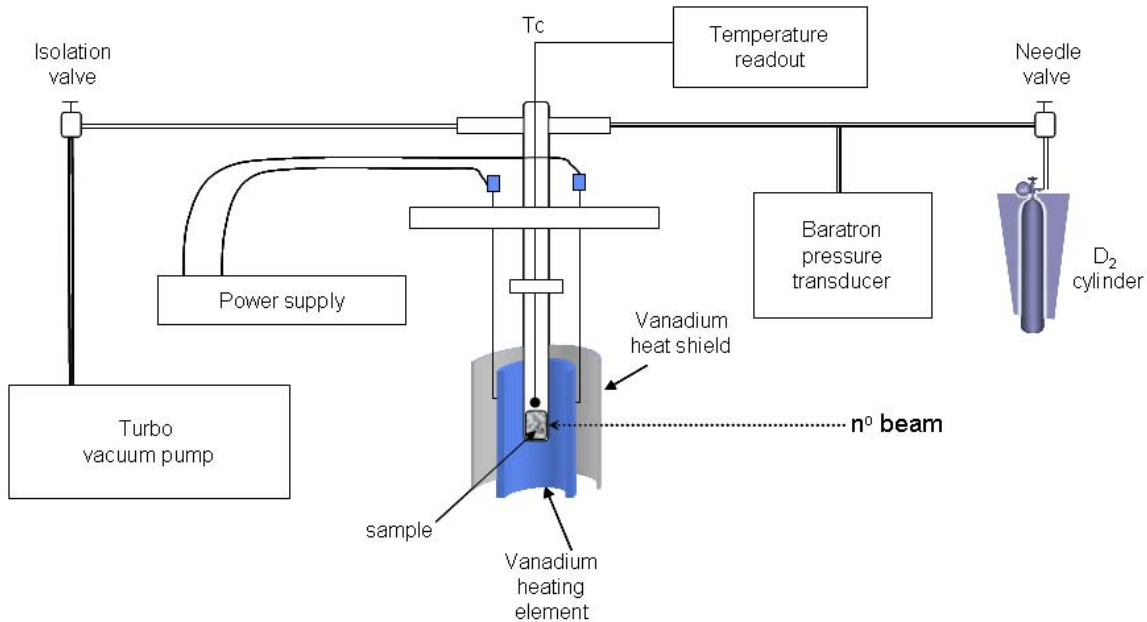


Figure 2. Schematic of the experimental setup for in-situ D_2 loading of Er metal.

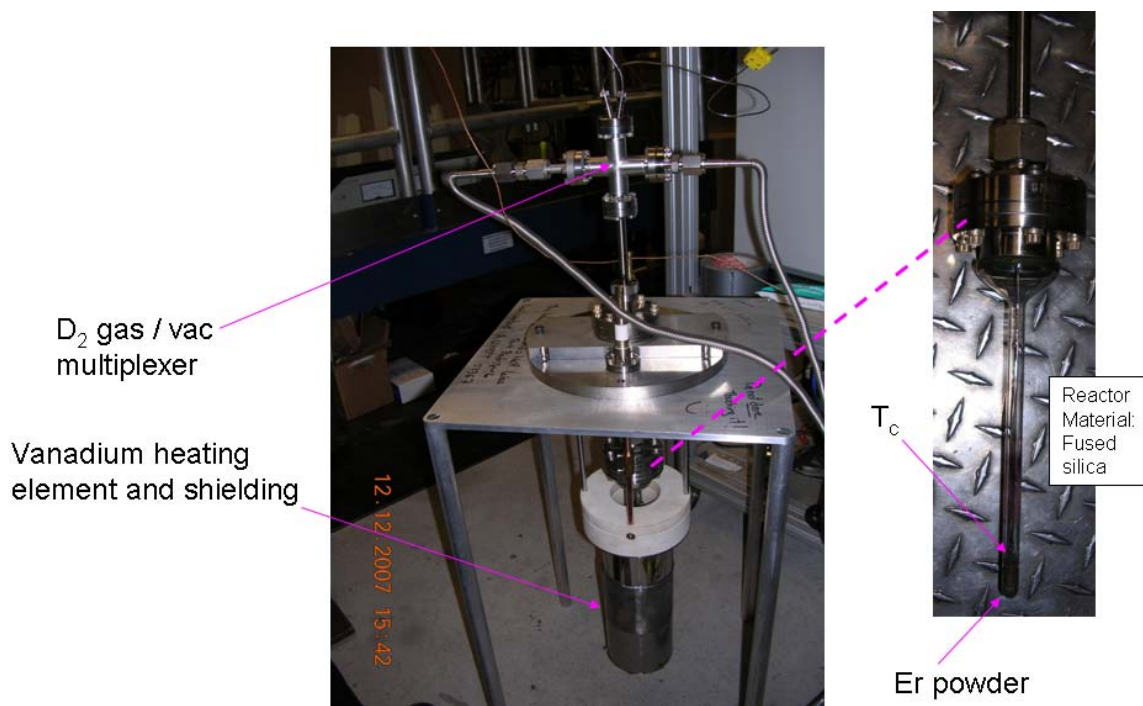


Figure 3. Actual setup of in-situ reaction vessel, heater, and gas handling system.

Figure 3 shows the actual setup of the reactor vessel, gas system, and heater prior to installation into the experimental chamber of the High Intensity Powder Diffraction (HIPD) beam-line at LANSCE. A close-up view of the reactor chamber is shown as well. The actual reactor vessel was fabricated from fused silica (~7 mm diameter). The reactor vessel was attached to a vacuum flange by a gas-to-metal seal. The flange was subsequently attached to the upper part of the gas system. The entire gas system could be adjusted up-and-down by a gasket at the top plate of the setup. This enabled height adjustment for optimal placement of the specimen in the neutron beam.

Figure 4 shows the entire experimental setup installed into the chamber at HIPD ready for neutron diffraction analysis. The large neutron scattering chamber (approx. 1 m³) of HIPD is typically evacuated to $\sim 10^{-5}$ Torr in order to reduce scatter and improve counting statistics during data collection. The vacuum conditions of the scattering chamber allowed straightforward use of the vanadium heating element without the concern for oxidation of the vanadium metal during heating for temperature values up to 700°C. Because the fused silica reactor vessel would experience various pressures on the internal walls of the reactor while simultaneously experiencing vacuum conditions of the neutron scattering chamber on the exterior reactor walls, a trial run was performed without the use of D₂ gas. This was accomplished by simply heating the empty reactor up to 600°C with the large HIPD chamber pumped to 10⁻⁵ Torr and atmospheric pressure (air) in the reactor and subsequent attached plumbing system. Various cycling of air and vacuum conditions inside the reactor, at temperatures ranging from 300-700°C showed that the

fused silica reactor was robust and easily handled pressure cycling. As our experiment did not plan to exceed 500 Torr D₂ pressures, testing to atmospheric pressure (i.e. ~ 600 Torr for Los Alamos, NM) was sufficient to establish functionality of the reactor under conditions expected during loading.

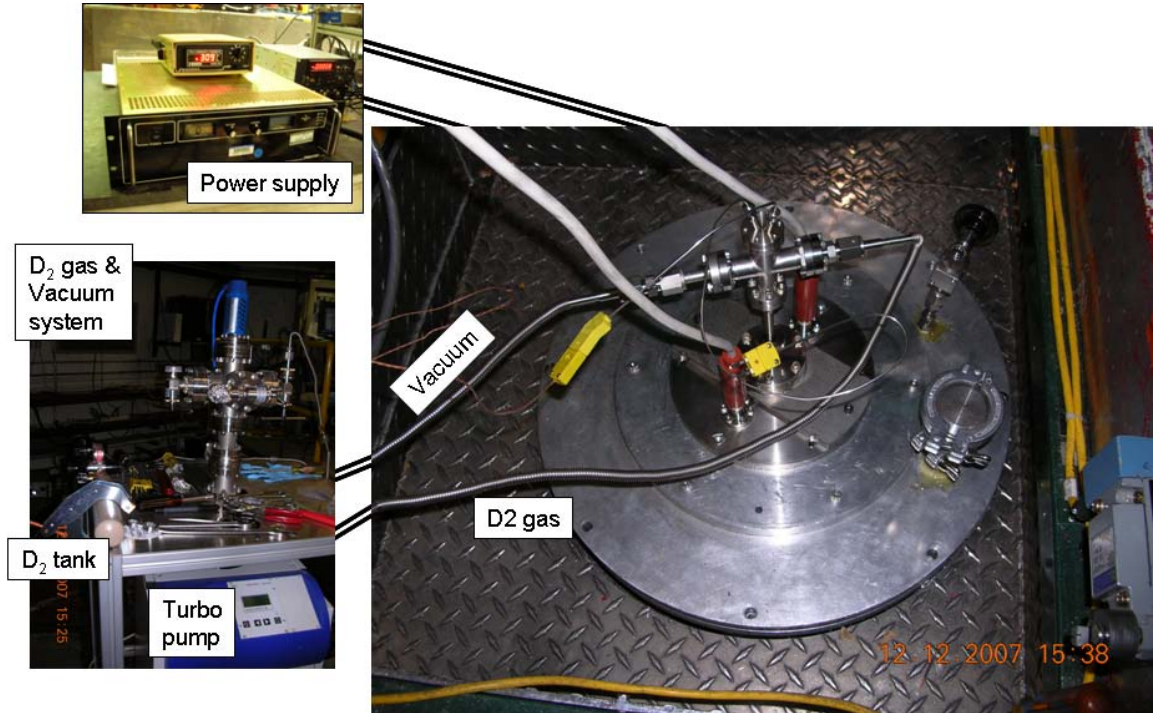


Figure 4. Actual experimental setup on the HIPD beam-line (LANSCE).

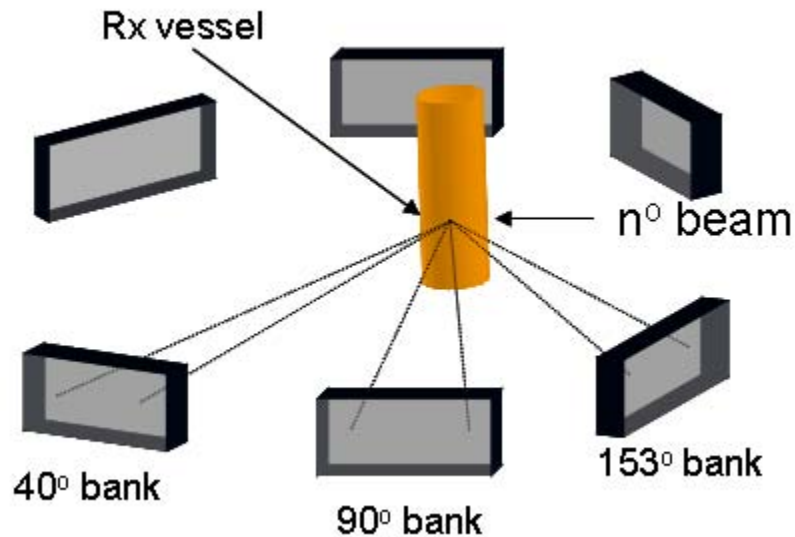


Figure 5. Schematic illustration of detector banks on HIPD relative to sample and neutron beam.

Figure 5 is a schematic regarding the positioning of detector banks during collection of neutron diffraction histograms from HIPD. The spectrometer has 6 detector banks as shown. These banks serve to obtain diffraction spectra from the sample. Note that because this is a time-of-flight (TOF) experiment, the specimen and detector banks are fixed. This reduces issues associated with data collection with respect to specimen and detector alignment. The lower angle (40°) banks have higher intensity with moderate resolution over a large range of d-spacing. The higher angle banks (153°) have better resolution but a more limited range of d-spacing and lower intensity. The 90° banks are intermediate in resolution and d-spacing range, as compared to the 40° and 153° banks, while still yielding good intensity. Use of multiple detector banks yields excellent results regarding phase fractions as well as structural parameters of the observed phases. All detector banks were used in the analysis.

Results and Discussion

Histograms shown in Figure 6 demonstrate the excellent refinement of experimental data. As one can see, the solid green line calculated from the structural model matches well to the observed patterns (plotted in red as individual + symbols). Note that a region in the 90° and 40° banks was removed due to scatter from the Silica reaction vessel. Otherwise, the patterns were free of experimental artifacts. Excellent residual error values ($R_p < 5\%$) were typical for our analysis, indicating the appropriateness of the structural models employed in the refinement. The difference patterns, shown at the bottom of each plot (purple), are also employed as a visual gauge for the quality of the fit and in these refinements the difference patterns were essentially flat. This suggests appropriate modeling of the observed histograms. This also lends credibility to the resulting refined structural parameters.

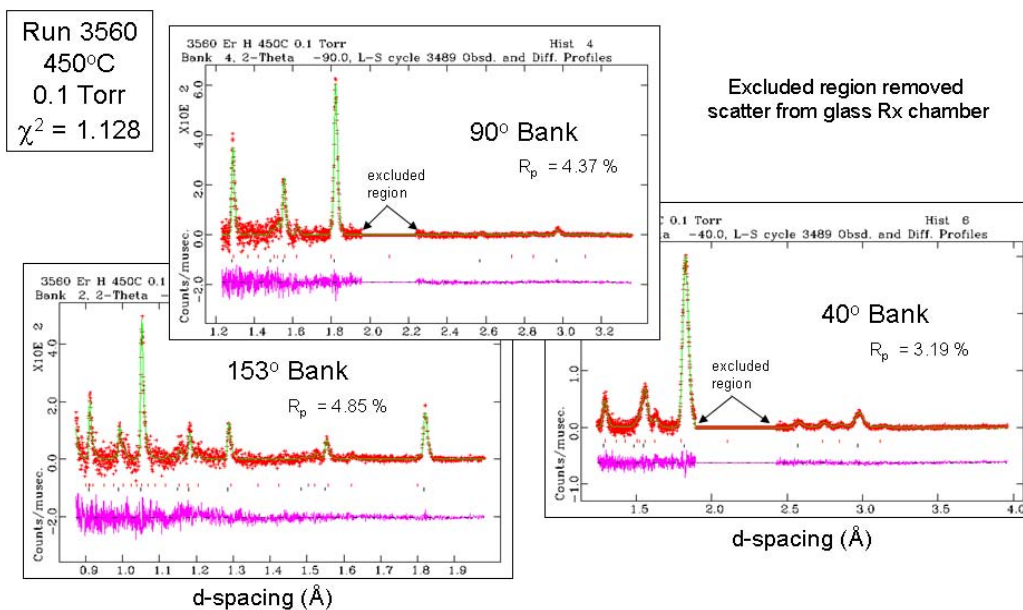


Figure 6. Rietveld refinement of experimental histograms from 40° , 90° , and 153° detector banks. See text for details.

To obtain an overall picture of the hydration process, a contour map was generated as shown in Figure 7. This plot (employing data from one of the 90° banks) represents the sequential plotting of histograms from the specimen at 450°C. The plot shows how the neutron diffraction pattern changes as various pressures of D₂ are bled in from the D₂ cylinder. At the onset of the experiment the Er powder was at vacuum conditions (~10⁻⁷ Torr) and held steady at 450°C. The histogram for Er is plotted at the bottom of the contour plot and is denoted by the label: No D₂. The hexagonal Er structure has its major peak (101) at ~2.7 Å as shown by the yellow band along the x-axis in the contour plot (yellow = high intensity, red = low intensity for contour plot). Over the course of about 20 hours D₂ gas was allowed to flow into the reaction vessel; first at 0.1 Torr, then 1.0 Torr, and finally 10 Torr and higher.

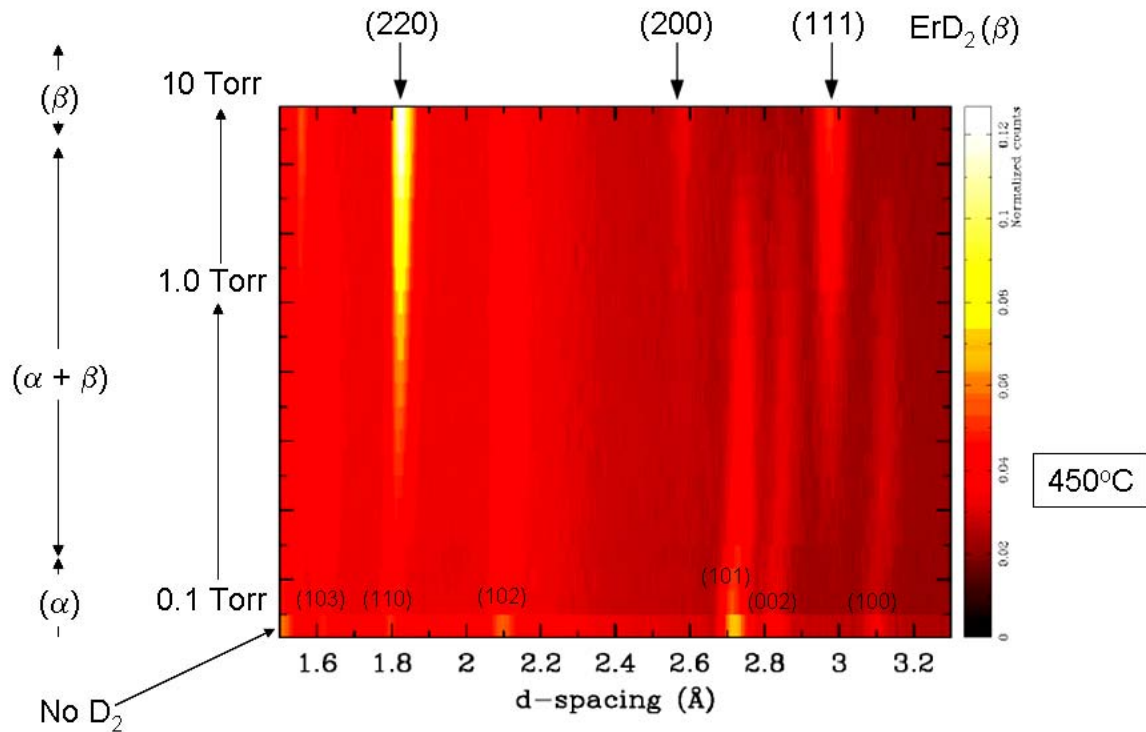


Figure 7. Contour plot illustrating in-situ formation of the α and β phases of erbium deuteride via D₂ loading at various pressures. Sample held at 450°C during D₂ loading. Red = low intensity, yellow = high intensity.

The contour plot shows how the Er pattern slowly expands (peaks shift to larger d-spacings) as deuterium is added into the reactor vessel. Initially, our observations at 0.1 Torr indicated the formation of only the α phase solid-solution. The α phase has the same structure as Er metal but with deuterium locating in the interstitial sites of the hexagonal lattice.[5] This is why the results only indicated shifting of peaks and not the loss of any observed hkl indices. With time, the specimen entered a two phase region of α phase along with the formation of the β (fluorite) ErD_{2-x} phase. This is clearly distinguished by the growth of the (111) peak of the β phase at ~3.0 Å. This peak is detectable roughly halfway through the 0.1 Torr exposure and grows dramatically with

increased D_2 pressures. As the reaction continued to progress with time and increased D_2 pressure, the β phase became the dominant phase fraction, until the sample fully converted to the ErD_2 fluorite as indicated by the strong (220) peak at $\sim 1.8 \text{ \AA}$ as well as the (200) and (111) reflections as labeled at the top of the contour plot.

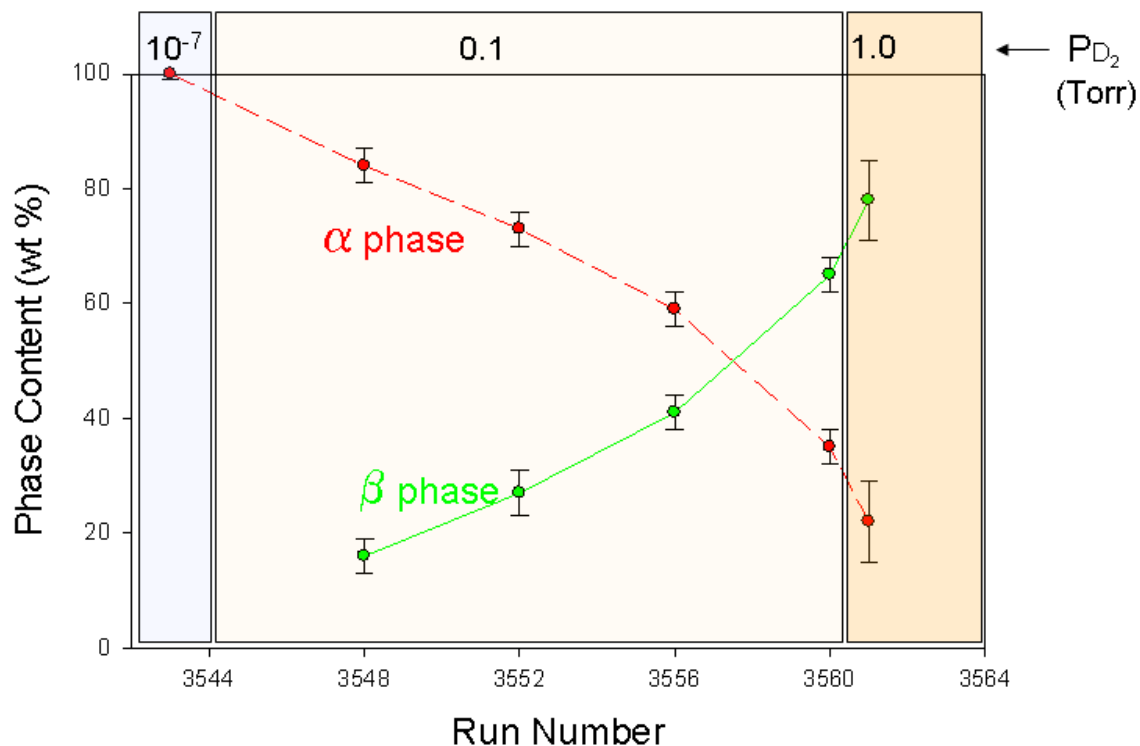


Figure 8. Weight fraction of α and β phases vs. Run Number for D_2 loading at $450^\circ C$.

Significant quantification of results could be obtained via Rietveld refinement. Table 3 documents various refined parameters for the α and β phases during loading. We document our results as a function of Run Number for purposes of bookkeeping and comparison of the progression of the reaction. However, the Run Number can be roughly translated as time where typical histogram collection runs required roughly 20 to 40 minutes. We show the phase fraction (wt %) of the α and β phases as a function of Run Number in Figure 8. In this plot the regions are highlighted based on the existing D_2 pressure present on the powder during each Run. The plot shows that the β phase becomes the majority phase in the reactor even at 0.1 Torr.

The setting of the D_2 pressure during analysis was typically performed by adjusting a needle valve controlling the D_2 gas until the pressure of the reactor read the desired D_2 loading pressure on the MKS Baratron readout. This pressure value tended to decrease over time as the D_2 gas was consumed by the Er powder in the reactor. Hence, the experiment required monitoring of the D_2 pressure and recurrent adjustments of the needle valve to keep the pressure near to its set-point. We chose to increase pressure to

1.0 Torr between run 3560 and 3561 because we had reached conditions where the D₂ gas pressure of 0.1 Torr stabilized over the Er powder. This may not have been a true thermodynamic equilibrium condition for the sample, as perhaps with more time the sample might have converted fully to ErD₂. However, at this point in our experiment it made sense to increase the D₂ pressure so that conversion to the β phase could be achieved in the limited time frame of the experimental beam-time.

Upon increase to 1.0 Torr, the conversion to β phase continued to progress with complete conversion to ErD₂ occurring at \sim 10 Torr D₂ (not shown on plot). We did not detect the presence of Er₂O₃ in the observed diffraction data. As mentioned earlier, the Er metal most assuredly contained an oxide passivation layer due to exposure of the metal to air. The lack of detection of Er₂O₃ would indicate that the passivation layer contributes an insignificant fraction of the measured intensity.

Table 3. Refined structural parameters for α and β phases during D₂ loading at 450°C.

Run #	PD ₂ (Torr)	Wt % α phase	a axis (Å)	c axis (Å)	cell vol. (Å ³)	Wt % β phase	a axis (Å)	cell vol. (Å ³)	Rp (%)
3543*	< 10 ⁻⁷	100	3.564(1)	5.627(1)	61.91				2.62
3548	0.1	84(3)	3.593(1)	5.681(1)	63.51	16(3)	5.140(1)	135.82	3.95
3552	0.1	73(3)	3.600(1)	5.693(1)	63.89	27(4)	5.141(1)	135.90	3.87
3556	0.1	59(3)	3.601(1)	5.698(1)	63.98	41(3)	5.142(1)	135.94	3.83
3560	0.1	35(3)	3.601(1)	5.697(1)	63.98	65(3)	5.142(1)	135.97	3.76
3561	1	22(7)	3.601(1)	5.700(1)	64.01	78(7)	5.142(1)	135.98	3.77
3565	1					100	5.142(1)	135.97	3.83
3566	10					100	5.142(1)	135.94	3.76

*Er metal under vacuum prior to exposure to D₂ gas

Parentheses next to numbers indicate 3 σ error on the last digit of value

Figure 9 shows results for the cell volume of the α and β phase as a function of Run Number. This plot reveals that the α phase undergoes rapid expansion upon exposure to D₂ gas. In contrast, the volume of the β phase changes very little during its growth in phase fraction. This implies that the β phase forms very near the stoichiometric ErD₂ composition and remains this way from its presence as a minor phase, until its full conversion. This observation suggests that substoichiometric ErD_{2-x} may be difficult to form using our employed loading procedure.

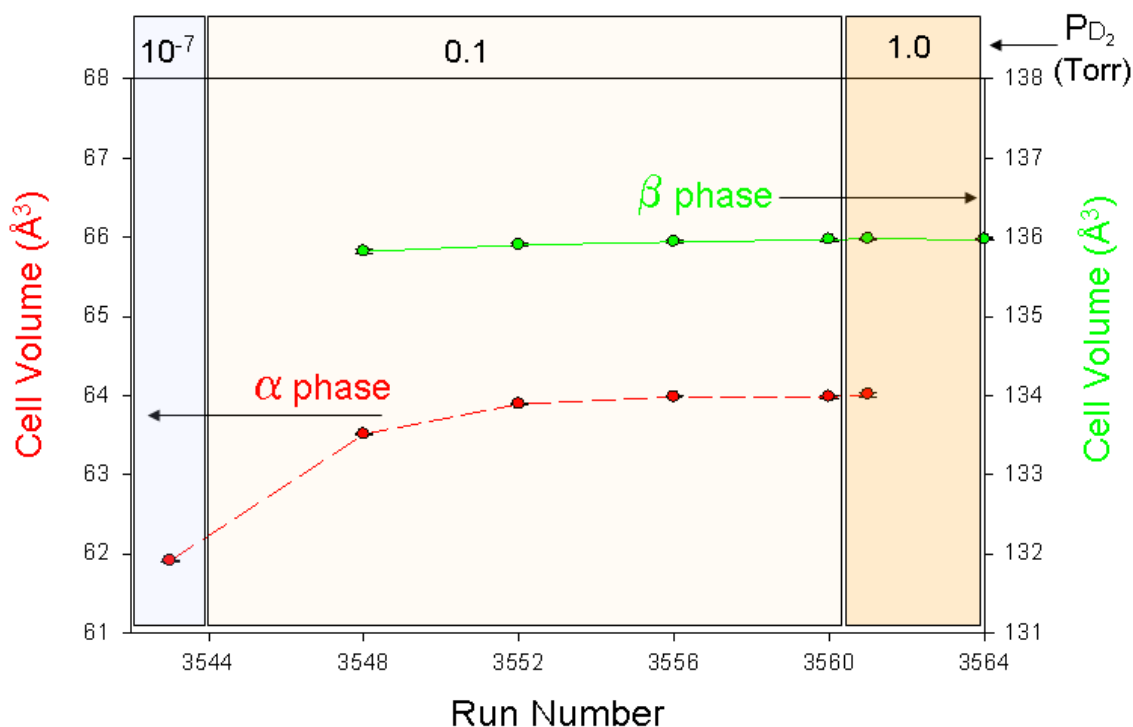


Figure 9. Unit cell volume for α and β phase vs. Run Number for D_2 loading at $450^\circ C$.

Once the sample had been fully converted to the β phase at ~ 10 Torr D_2 our analysis indicated that the D_{tet} sites of the fluorite were completely filled, with essentially no deuterium occupying the D_{oct} site locations (see Figure 1, Model 2). By further increasing the D_2 loading pressure above 10 Torr, we could test for the possible presence of D_{oct} in the β phase at $450^\circ C$. Run Numbers 3590 and 3592 employed overpressures of 200 and 500 Torr, respectively. Table 4 documents the resulting structural changes that occurred with these overpressures. Our analysis indicated the presence of D_{oct} site occupancy for both the 200 and 500 Torr overpressures at occupancies of 5% and 9%, respectively. Figure 10 graphically displays the results of occupancy refinement for D_{tet} and D_{oct} sites. After completion of the data collection for the 500 Torr overpressure (Run Number 3592), the D_2 gas was vacuum pumped out from the reactor while maintaining the sample at $450^\circ C$.

Table 4. Refinement parameters for ErD_{2+x} with D_2 overpressure & vacuum ($450^\circ C$).

Scan #	T ($^\circ C$)	P (Torr)	ρ (g/cm^3)	a (\AA)	vol (\AA^3)	Er B_{iso} (\AA^2)	D_{tet} site occ.	$D_{tet} B_{iso}$ (\AA^2)	D_{oct} site occ.	$D_{oct} B_{iso}$ (\AA^2)	Er D_7
3567	451	13.2	8.367	5.1419(2)	135.95(2)	1.66(2)	0.99(1)	2.1(1)	0	-	1.98
2590	453	198.1	8.379	5.1412(2)	135.89(2)	1.58(2)	1.01(1)	2.2(1)	0.05(1)	7(2)	2.07
3592	454	500.6	8.382	5.1413(1)	135.90(1)	1.58(2)	1.01(1)	2.2(1)	0.09(1)	9(2)	2.11
3593	455	<10-4	8.365	5.1425(1)	135.99(2)	1.58(2)	1.00(1)	2.3(1)	0	-	2.00
3594	455	<10-7	8.364	5.1432(2)	136.05(2)	1.50(2)	1.01(1)	2.4(1)	0	-	2.02

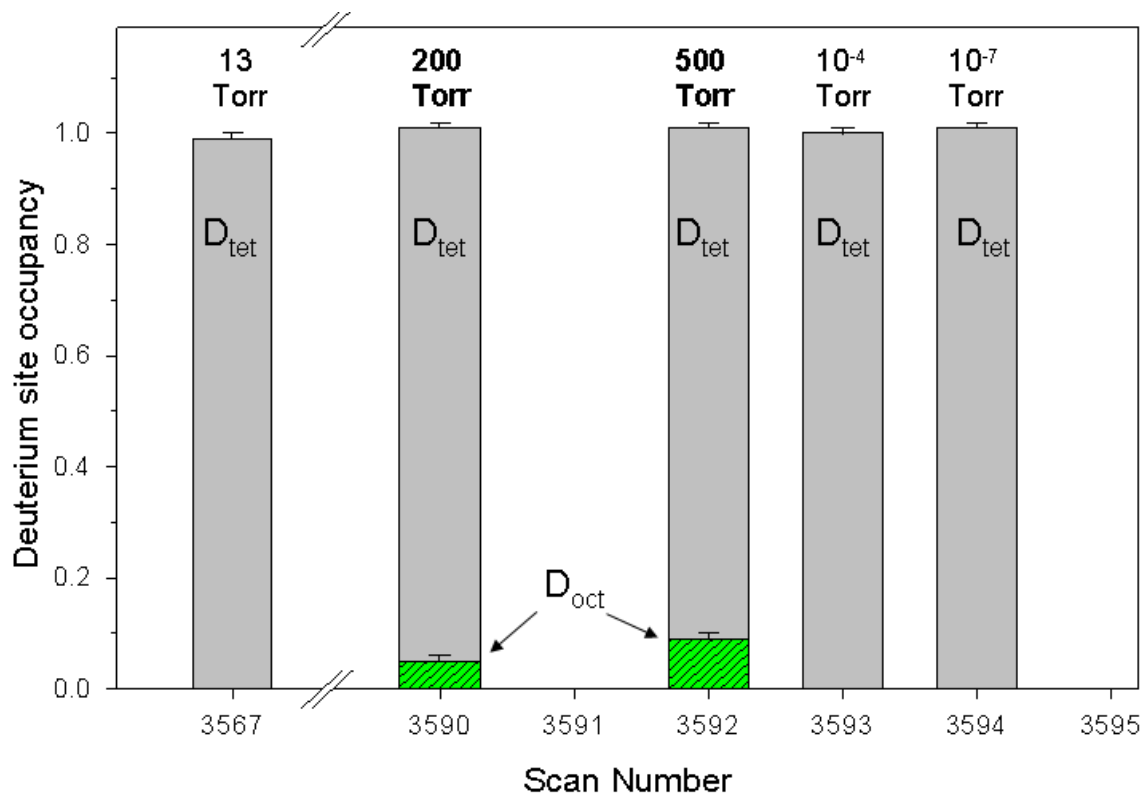


Figure 10. Deuterium occupancy for D_{tet} and D_{oct} sites in β phase erbium deuteride under various conditions of D_2 pressure/vacuum (Temperature = 450°C).

Two additional Runs were collected during the process of evacuating the reactor. Run Number 3593 was collected while the chamber was in the process of pumping; the average pressure during this run was $\sim 10^{-4}$ Torr. Run Number 3594 was collected after the vacuum system had pumped the reactor down to 10^{-7} Torr. An important result of our in-situ analysis is that the D_{tet} sites maintain complete occupancy at 450°C , even after pumping to high vacuum conditions. In contrast, the D_{oct} sites are completely evacuated by the pumping process. The loss of the D_{oct} sites via pumping can be explained by the fact that these sites are very unstable. As discussed earlier, the D_{oct} sites coordinate to D_{tet} as their nearest neighbors. While the deuterium is quite stable in the preferred D_{tet} site, location on the D_{oct} site is not preferred.[6] Only with significant overpressures of D_2 gas at high temperatures will deuterium locate at the D_{oct} site, and indications are that it is quite unstable. The B_{iso} values (B_{iso} being a measure of thermal motion) shown in Table 4 indicate that the D_{tet} sites range from 2.1 - 2.4 \AA^2 . In comparison, the much heavier Er atom shows only slightly smaller values (1.5 to 1.7 \AA^2). However, for the case of D_{oct} the B_{iso} values jump to 7 and 9 \AA^2 for 200 and 500 Torr, respectively. Clearly there is a difference in stability between these two sites at 450°C that suggests difficulty in loading of the D_{oct} site and ease of removal of D_{oct} occupancy while maintaining the more stable D_{tet} occupancy.

Conclusions

In-situ neutron diffraction yields structural information regarding deuterium loading for Er metal at 450°C. The α phase shows dramatic cell expansion upon exposure to D₂. The β phase shows little structural change in the ($\alpha + \beta$) two-phase region. This suggests formation of the β phase near ErD₂ stoichiometry. D₂ overpressures of 200 to 500 Torr indicate 5 to 9 % occupation of D_{oct} sites, respectively. Pumping to vacuum (i.e. below 10⁻⁴ Torr) at 450°C revealed removal of D_{oct} sites with no reduction of D_{tet} sites, thereby forming fully D_{tet} occupied β phase (ErD_{2.0}). No erbium oxide (Er₂O₃) phase was detected in our neutron diffraction results. Our analysis yielded the necessary D₂ pressure for loading of Er metal while at 450°C (i.e. ~10 Torr). Overpressure to as high as 500 Torr D₂ followed by pumping to vacuum (< 10⁻⁷ Torr) was not detrimental to the formation of stoichiometric β phase ErD_{2.0}.

References

- [1] C. E. Lundin, *Trans. Metall. Soc. AIME* **242** (1968) pp. 903 & 1161.
- [2] C. R. Tewell and S. H. King, "Observation of metastable erbium trihydride" *Applied Surface Science*, **253** (2006) pp. 2597-2602.
- [3] SAND 2007-8105 "PCT Apparatus: Overview" by R. Ferrizz, T. J. Louck and S. H. King.
- [4] T. J. Udovic, J.J. Rush and I. S. Anderson, "Neutron spectroscopic evidence of concentration-dependent hydrogen ordering in the octahedral sublattice of β -TbH_{2+x}" *Phys. Rev. B*, **50** (1994) pp.7144.
- [5] C. K. Saw, B. J. Beaudry and C. Stassis, "Location of deuterium in α -scandium" *Phys. Rev. B*, **27** (1983) pp.7013.
- [6] R. R. Wixom, J. F. Browning, C. S. Snow, D. R. Jennison, and P. A. Schultz, "First principles site occupation and migration of hydrogen, helium, and oxygen in β -phase erbium hydride" *J. Appl. Phys.* to be published (2008).

Distribution:

1	MS 0871	C.L. Renschler, 2730
1	MS 0878	M.O. Eatough, 2735
1	MS 0878	L.I. Espada, 2735
1	MS 0878	R.M. Ferrizz, 2735
1	MS 0878	D.R. Kammler, 2735
3	MS 0878	C.S. Snow, 2735
1	MS 0869	C.A. Papp, 2739
1	MS 0862	C.C. Busick, 2713
1	MS 0863	S.H. King, 2713
1	MS 1361	C.R. Tewell, 6754
3	MS 1411	M. A. Rodriguez, 1822
1	MS 1455	R. R. Wixom, 2555
1	MS 0899	Technical Library, 9536 (electronic copy)

